Three-Dimensional Supersonic Homogeneous Turbulence: A Numerical Study

D. H. Porter,[1] A. Pouquet,[2] and P. R. Woodward[1]

[1]*Department of Astronomy and Minnesota Supercomputer Institute, University of Minnesota, Minneapolis, Minnesota 55415*

[2]*Observatoire de la Côte d'Azur, 06003 Nice CEDEX, France*

(Received 21 June 1991)

A turbulent homogeneous perfect gas with no forcing is computed using the piecewise-parabolic method on a uniform gird of 256^3 zones. The initial rms Mach number is one. The main results are (i) persistence of a quasisupersonic phase with strong density contrasts over several shock formation times; (ii) late appearance of a post-supersonic self-similarly decaying regime in which the total velocity spectrum varies with wave number as k^{-1}; and (iii) both shock curvature and velocity gradients are important mechanisms of vorticity production in the first half of the supersonic phase.

PACS numbers: 47.10.+g, 47.40.Ki

The investigation of compressible turbulence is of fundamental importance to a number of research areas in fluid dynamics. In astrophysics, compressible turbulence is likely to play an important role in the process by which stars are formed from dense clouds of interstellar gas, in particular, in slowing down the collapse. In aeronautical engineering, compressible turbulence occurs in the wakes of supersonic projectiles and may play an important role in the design and operation of scramjet engines.

Most of the analytical and numerical studies in three dimensions on turbulent compressible fluids are confined to the subsonic regime [1]. We report here the most significant results obtained using the piecewise-parabolic method (PPM) [2], on a uniform mesh of 256^3 zones of size Δx, for a turbulent decaying flow at an initial rms Mach number of unity.

Our model equations are the fluid dynamical equations for a perfect gas without macroscopic dissipation for the fluid velocity $\mathbf{u}$ and internal energy e, together with the continuity equation for the density ρ. The sound speed is $c^2=\gamma(\gamma-1)e$ and we take $\gamma=1.4$. Direct measurements of PPM's numerical damping of sinusoidal shear fields [3] indicate an effective numerical viscosity which varies with wavelength $\lambda=\sqrt{2}L_0$ and Mach number M as $\nu_{\rm eff}/c\lambda=0.462(M+\frac{1}{4})^{3.15}(L_0/\Delta x)^{-3}$. This form of $\nu_{\rm eff}$ assumes a dominant mode. Direct measures of PPM's dissipation [3] show that weak waves (advected by larger modes) decay by a factor of $1/e$ after they have traversed a distance which scales as $(\lambda/\Delta x)^{3.5}$ times their own wavelength λ. In particular, a mode with $\lambda=10\Delta x$ decays by $1/e$ after it has traversed 100λ.

We choose units so that the mean density ρ_0 and initial mean sound speed c_0 are both unity. Boundary conditions are periodic in the three principal directions of the cubical computational domain. The initial conditions are random and independent fluctuations in the velocity, density, and pressure with spectrum: $E(k)\sim k^4 e^{-2(k^2/k_0^2)}$, where $k_0=2$. Modes are initially excited up to $k=32$. We set the initial rms fluctuations in the density $\delta\rho=(\rho-\rho_0)/\rho_0$, pressure $\delta p=(\rho e-\rho_0 e_0)/\rho_0 e_0$, and velocity δU_0 to 20%, 20%, and 1%, respectively. The initial density contrast $\Delta\rho=\rho_{\rm max}/\rho_{\rm min}$ is close to 4. Other sets of initial conditions tested both in 2D and in 3D at lower resolutions, with PPM as well as Navier-Stokes solvers [4], indicate a lack of sensitivity of the results in a wide range of initial parameters.

This numerical simulation, run Q42, was performed on a 256^3 mesh, and allowed to evolve through a time $t=3.2\tau_{\rm ac}$, where $\tau_{\rm ac}$ is the acoustic time of the energy-containing scale and is the unit of time for these computations. In the unperturbed flow, a sound wave takes 2 time units to cross the domain of our simulation. We define $\mathcal{K}_{n,x}$ as the wave numbers associated with the compressional ($x=c$), solenoidal ($x=s$), and total ($x=v$) components of the velocity field $\mathbf{u}=\mathbf{u}^s+\mathbf{u}^c$:

$$\mathcal{K}_{n,x}=\left\langle \int_0^\infty k^n E^x(k)dk \Big/ \int E^x(k)dk \right\rangle^{1/n},$$

where E^x are the power spectra of the c component, s component, and total velocity. The ratio $\chi=E^c/E^v$ (compressional/total) is yet another parameter of the initial conditions; we take $\chi\sim 9\%$.

Temporal evolution of a supersonic flow.— In the absence of a source term, the kinetic energy of a compressible flow decays inexorably as a consequence of shock formation and dissipation of small scale eddies produced by vortex stretching. In our simulations dissipation on small scales is due to the finite mesh, in real systems dissipation is typically due to molecular diffusion. After a first period of nonlinear wave steepening and mode coupling the subsequent decay of kinetic energy appears to take place in *two distinct quasisteady phases* separated by a short transitional period: first, a compressional period dominated by shock formation and shock interactions, and second, a period dominated by vortex interactions and vortical decay. This is revealed in the temporal evolution of several small-scale variables such as $\mathcal{K}_n$ or the density contrast $\Delta\rho$. As seen, e.g., in the Taylor wave numbers (Fig. 1) first is a period of rapid growth, up to $t_1\sim 0.3$. This onset phase corresponds to the formation of shocks which, as coherent nonlinear structures, feed compressional modes of all wave numbers at the same

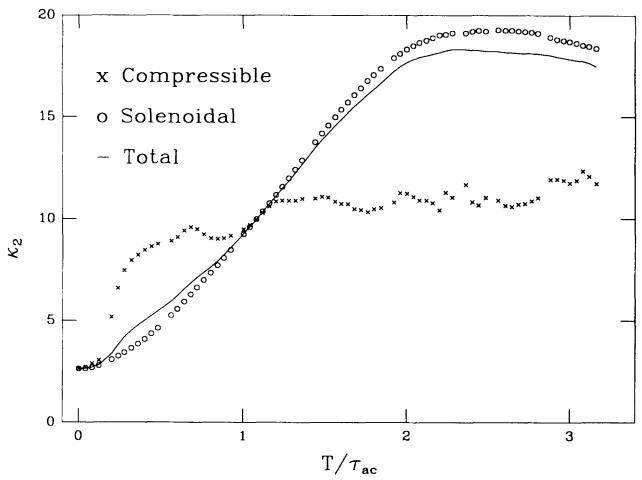

FIG. 1. Temporal evolution of the characteristic Taylor wave number $\mathcal{K}_2$ separated into its solenoidal (circles), longitudinal (crosses), and total (solid line) components. Note the onset of the quasisteady supersonic phase on $\mathcal{K}_c$ at $t_1 \sim 0.3$ and that of the post-supersonic phase on $\mathcal{K}_s$ at $t_2 \sim 2.1$.

time. At $t \sim t_1$, the density fluctuations $\delta\rho$ reach a value of 52%, the density contract $\Delta\rho \sim 60$, and $\rho_{\min} = 0.14$. From t_1 onward, the compressional mode $\mathcal{K}_{2,c}$ is roughly constant. Next is a quasisteady supersonic phase for $t_1 < t < t_2$ with $t_2 \sim 2.1$, during which the solenoidal modes, represented by $\mathcal{K}_{2,s}$, continue to grow, more slowly than the compressional component, and the density contrast remains at a high value, on average 45, with local fluctuations due to the presence of many strong shocks and their interactions. During this second phase a roughly linear growth for $\mathcal{K}_{n,s}$ occurs, at a rate which increases with n for $n = 1$, 2, 3, and 4. For $n > 4$, $\mathcal{K}_{n,s}$ increases abruptly at time t_1, and then increases at a rate independent of n until time t_2. During this second phase local regions of supersonic flow can be found. Finally we have a post-supersonic phase in which the Mach number is substantially lower than unity.

During this third phase, both the density contrast $\Delta\rho$ and the density fluctuations $\delta\rho$ are much smaller ($\Delta\rho \sim 4$ and $\delta\rho \sim 0.15$ at $t_{\max} = 3.2\tau_{ac}$), and the characteristic wave numbers $\mathcal{K}_n$ are roughly constant in time. Comparisons with similar simulations [4] run on 64^3, 128^3, and 256^3 meshes indicate that (i) the saturated values of $\mathcal{K}_n$ increase with mesh resolution, as they would increase with Reynolds number in a Navier-Stokes system; these wave numbers indicate the scales at which various derivatives of the velocity are important for the simulation at hand; (ii) the relative dominance of the compressive or solenoidal modes at high wave numbers, as well as the times at which $\mathcal{K}_n$ abruptly change and saturate (namely, t_1 and t_2), are essentially independent of the mesh resolution.

The initially imposed dominance of solenoidal modes is recovered after a short period of time during which the compressional modes overpower the solenoidal ones in the small scales due to strong and rapid shock formation preceding slower vortex formation. After shocks form the rms Mach number, M_a, initially equal to 1.1 with excursions up to $M_{\max} \sim 6.2$, decays steadily and linearly during $t \in [0.4, 2.0]$. M_a is below unity on average after $t \sim 0.6$. At the final time of the computation, $t_{\max} = 3.2\tau_{ac}$, $M_a = 0.36$, but the maximum local Mach number is still $M_{\max} = 1.5$, as can be inferred from histograms [4]. In fact, at $t_{\max}$ supersonic flow fills 0.03% of the volume distributed in several dozen small regions.

The time for compressional modes to develop fully is considerably shorter than the time for the solenoidal modes to develop in the system examined here. This disparity is clearly seen in the Taylor scales shown in Fig. 1. In fact, all of the compressional modes jump simultaneously from their initial small values (essentially zero for $k > 5$) to within 86% of their peak values during $t \in [0.3t_1, t_1]$: All compressional modes are excited together when shocks form by time t_1. The solenoidal modes grow more slowly and at different times: Solenoidal modes of shorter wavelengths take longer to reach their peak amplitudes than do those of longer wavelengths, indicative of a forward cascade of energy. The time for all of the solenoidal modes to develop fully seems to be linked with the eddy rotation time of the energy containing scale, which is close to t_2.

Given our initial conditions, and for almost any supersonic and random initial conditions, the entire velocity field (not just the initially compressional component) contributes to shock formation. In general, a random pressure field is not consistent with stable eddies. Further, in run Q42 variations in the pressure field are about 6 times too small to support stable eddies. Hence the initial energy in the solenoidal field is quickly converted into compressional energy as elements of gas moving in roughly straight lines collide. In order for an eddy to equilibrate, there must be enough time for the eddy to turn over at least once. However, in order for a shock to develop, two parts of a flow moving in opposite directions at supersonic speeds need only move a fraction (less than half) of their initial distance of separation. The distance of half of the energy containing scale corresponds to both a typical eddy's diameter and the typical initial separation of elements of gas that collide energetically. Both sets of motions come from the same random velocity field, so they typically have similar amplitudes. Hence, the ratio between the time of shock formation and the time of eddy formation is roughly the ratio of the distances given above, which is the ratio of the radius of a circle to its circumference; in fact, $t_2/t_1 \sim 7$.

Characteristic structures of a decaying supersonic flow.—The temporal evolution of the solenoidal $E^s(k)$ and compressional $E^c(k)$ components of the velocity power spectra follow the integrated variables we have described above. Small scales develop as the flow evolves. E^c settles to the form k^{i_c} at $t \sim t_1$ and then decays nearly

self-similarly, with a spectral index $i_c \sim 2.04 \pm 0.17$ on average for $t \in [0.3,2.1]$. However, the evolution of E^s is much slower: A self-similar regime occurs only after $t \sim t_2$. The total spectrum is dominated at all scales, except for a short time early in the quasisupersonic phase, by its solenoidal component.

We calculated the averaged spectra in the quasisupersonic phase $t \in [0.3,2.1]$ and in the post-supersonic phase, $t \in [2.1,3.2]$. Assuming that this averaging procedure is justified, the spectral indices in the former phase are close to 2 for all velocity spectra, as is expected for a discontinuity, the structure that must be dominant during that time. However, in the last phase, shown in Fig. 2, with the s, c, and v components denoted by circles, crosses, and the solid curve, respectively, the spectral indices differ: Whereas the compressional component retains a rather steep spectrum, $i_c \sim 1.74 \pm 0.17$, the solenoidal component has an index $i_s \sim 0.89 \pm 0.27$. These spectral indices are taken for $k \in [5,25]$, and the error bars stem from convergence studies [3]. Both convergence studies and direct measures of numerical damping rates [3] indicate that the mode amplitude of waves spanning $10\Delta x$ are in error by $\sim 17\%$ (corresponding to a 34% error in mode energy). Numerical errors have a smaller effect on all longer wavelength modes, and numerical dissipation increases rapidly and dominates as wavelength decreases from $10\Delta x$. In the simulation presented here, $10\Delta x$ corresponds to a wave number of $k \sim 25$, and we identify $k = 25$ as being roughly the border between the inertial and numerical dissipation ranges in run Q42.

The total velocity spectrum is quite flat during the final period. This may be a result of our limited grid resolution; it may also be due to hysteresis: The history of a supersonic phase in a now-subsonic flow leaves traces. This effect was already encountered in our 2D computations, where filamentary structures in entropy, density, and vorticity were observed at late times [4], with strong local vortices superimposed onto warped vorticity sheets [5]. It is also reminiscent of the spectrum of a passive scalar advected by an incompressible flow.

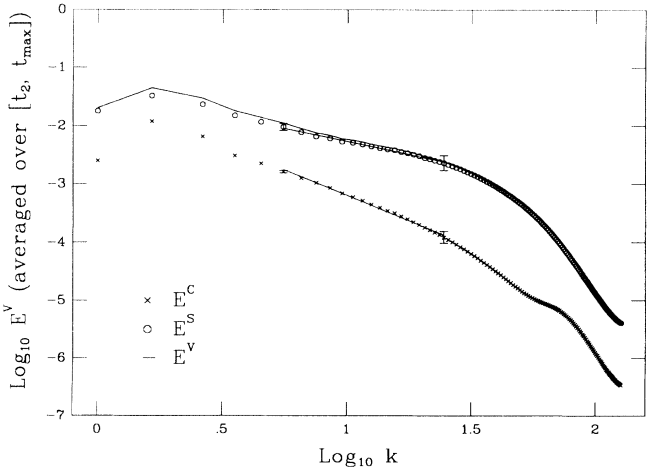

FIG. 2. Velocity spectra averaged over the time span $[t_2-t_{max}]$. The compressional, solenoidal, and total components are denoted respectively by crosses, circles, and a solid curve. The power-law fits $E^s \sim k^{-0.95}$ and $E^c \sim k^{-1.8}$ are shown as straight lines. The error bars shown are based on convergence studies of PPM.

The comoving evolution of vorticity is given by $d\omega/dt = \mathbf{B} + \mathbf{S}$, with the inhomogeneous baroclinic term $\mathbf{B} = (\nabla\rho \times \nabla p)/\rho^2$ and the linear in ω (stretching and compression terms) $\mathbf{S} = (\omega \cdot \nabla)\mathbf{u} - \omega(\nabla \cdot \mathbf{u})$. From inspection of the histograms of both $\mathbf{S}$ and $\mathbf{B}$, we infer that in the early supersonic phase, the baroclinic and the linear terms are roughly balanced [4]. This indicates that vorticity production through shock curvature (including intersecting shocks) is as important as the linear term in run Q42.

To assess the relative importance of $\mathbf{S}$ and $\mathbf{B}$, we also analyze the power spectra of their norms [4]. We find $B < S$ most of the time and for most scales. However, the two terms are comparable during the time of initial growth of the velocity—up to when the compression first becomes stationary ($t \sim t_1$). The linear term dominates later on. In an initially supersonic flow, the baroclinic term acts as a trigger of vorticity production on small scales: Intersecting shocks plant the seed of vorticity at short wavelengths which then undergo an exponential growth via the linear terms during the intermediate phase $t_1 < t < t_2$. Vortex sheets are established at shock intersections, and these sheets subsequently roll up due to the familiar shear instabilities. These vortex tubes are also unstable and are disrupted by kink instabilities, in which the phenomenon of vortex stretching plays a major role. This sequence of events is most clearly revealed in animations of volume rendered images of the flow which we have generated in our "numerical laboratory" [4].

A wide distribution of vorticity is generated during the first half of the simulation. At $t = 1.48$ the average and rms vorticities are 47.1 and 60.0; initially these values are 13.0 and 14.1, respectively. Vorticity decays in the second half of the simulation: By $t = 2.96$ the average and rms vorticities are 35.9 and 42.2, respectively. At $t = 2.96$, each component of vector vorticity is exponentially distributed. At earlier times, during which the system undergoes rapid evolution, the vorticity distribution is more complicated.

Even though the flow is subsonic at late times there are still entropy fluctuations due to shocks set up by high Mach number initial conditions [4]. The slow rate at which the entropy homogenizes is a measure of PPM's low numerical diffusion [3]. Entropy fluctuations, with their associated density fluctuations, make our flow (even at late times) violate the assumption of nearly uniform density which is typically made in analytical studies of low Mach number flow [6]. Thus, the arguments leading to steepening of the classical $-\frac{5}{3}$ Kolmogorov spectrum through coupling of vortices to acoustic waves may not

apply here.

In conclusion, in this paper we have shown the existence of two distinct temporal phases in the decay of an initially supersonic flow: a quasisupersonic phase in which many strong shocks interact, creating substantial vorticity, and a post-supersonic phase during which the energy spectrum, dominated by its vortical component, decays in a self-similar way following a shallow spectrum close to k^{-1}. The mechanism by which vorticity is produced in a supersonic flow differs in a substantial way from that in a subsonic or incompressible flow. In the supersonic case, phase-coherent shocks rapidly grow, so that the flow does not evolve under the same conditions as random vortex stretching, which is expected to be dominant in an incompressible flow.

More data analysis is in progress, in particular concerning correlations between density, entropy, and vorticity, a striking phenomenon in the 2D context [4], and questions motivated by incompressible studies: correlations between strain tensor and vorticity, exponentially distributed small-scale variables indicating intermittency, and the persistence of large-scale vortex filaments [7]. A detailed description of the characteristic structures, with 3D graphics in particular, that emerge in a turbulent compressible flow is beyond the scope of this paper and is being tackled elsewhere [4]. An *initially low* Mach number run will help us examine the nature of a subsonic flow, and help assess the long term effects of entropy structures produced by strong shocks.

Computations were performed at the Minnesota Supercomputer Institute on a Cray-2. This work was supported at the University of Minnesota by Grants No. DE-FG02-87ER25035 from the Office of Energy Research of the DoE, No. AST-8611404 from the NSF, the Air Force Office of Scientific Research (No. AFOSR-86-0239), and the ARO (No. DAAL03-89-C-0038) funding the Army High Performance Computing Research Center. At Nice, this work was supported by DRET (500-276), by the GDR-MFN, and by grants from the Observatory de la Côte d'Azur which is a CNRS URA 1362. We are also most grateful to T. Varghese for his assistance, and to T. Passot and P. L. Sulem for useful discussions.

[1] W. J. Feireisen, W. C. Reynolds, and J. B. Ferziger, thesis, Stanford University Report No. TF-13, 1981 (unpublished); G. Erlebacher, M. Y. Hussaini, H. O. Kreiss, and S. Sarkar (to be published); S. Kida and S. A. Orszag, J. Sci. Comp. **5**, 85–125 (1990); T. Passot and A. Pouquet, Eur. J. Mech. B/Fluids **10**, 377 (1991); T. A. Zang, R. B. Dahlburg, and J. P. Dahlburg, NASA Langley report, 1991 (to be published); S. Lee, S. K. Lele, and P. Moin, Phys. Fluids A **3**, 657 (1991).

[2] P. Colella and P. R. Woodward, J. Comput. Phys. **54**, 174 (1984); P. R. Woodward and P. Colella, J. Comput. Phys. **54**, 115 (1984); P. R. Woodward, in *Astrophysical Radiation Hydrodynamics*, edited by K.-H. Winkler and M. L. Norman (Reidel, Dordrecht, 1986).

[3] D. H. Porter, P. R. Woodward, and Q. Mei, Video J. Eng. Res. **1**, 1–24 (1991); D. H. Porter, P. R. Woodward, W. Yang, and Q. Mei, in *Nonlinear Astrophysical Fluid Dynamics*, edited by R. Buchler [Ann. N.Y. Acad. Sci. **617** (1990)].

[4] D. H. Porter, A. Pouquet, and P. R. Woodward (to be published); in *Supersonic Homogeneous Turbulence*, edited by J. D. Fournier and P. L. Sulem, Lecture Notes in Physics Vol. 392 (Springer-Verlag, Berlin, 1991), p. 105.

[5] T. Passot, A. Pouquet, and P. R. Woodward, Astron. Astrophys. **197**, 228 (1988); T. Passot and A. Pouquet, J. Fluid Mech., **181**, 441 (1987).

[6] S. S. Moiseev, V. I. Petviashvili, A. V. Tur, and V. V. Yanovskii, Physica (Amsterdam) **2D**, 218 (1981).

[7] R. H. Kraichnan, Phys. Rev. Lett. **65**, 575 (1990); W. Polifke, Phys. Fluids A **3**, 115 (1991); O. N. Boratav, R. B. Pelz, and N. J. Zabusky, Rutgers University report, 1991 (to be published); A. Vincent and M. Meneguzzi, J. Fluid Mech. **225**, 1 (1991).